Int. J. Multiphase Flow Vol. 16, No. 3, pp. 407–419, 1990
Printed in Great Britain.

0301-9322/90 $3.00 + 0.00

EXPERIMENTAL SIMULATION AND ANALYTICAL MODELING OF TWO-PHASE FLOW UNDER ZERO-GRAVITY CONDITIONS

L. P. WANG,[1] V. P. CAREY,[1] R. GREIF[1] and D. ABDOLLAHIAN[2]
[1]Department of Mechanical Engineering, University of California, Berkeley, CA 94720, U.S.A.
[2]S. Levy Inc., Campbell, CA 95088, U.S.A.

(*Received* 14 *February* 1989; *in revised form* 9 *November* 1989)

Abstract—A series of experiments are described in which an attempt was made to simulate two-phase flow behavior under zero-gravity conditions by the flow of two immiscible liquids of nearly equal densities. Pressure drop and void fraction data were obtained for the steady flow of two different liquid pairs for widely varying flow conditions. The two-phase flow in these experiments was in either the bubbly or annular flow regime. Values of the two-phase multiplier and void fraction obtained from the measured data were found to correlate well in terms of the Martinelli parameter X_{tt}, but the resulting variations of these parameters with X_{tt} differs significantly from the well-known correlation of Martinelli for these quantities. An analytical study of annular flow under zero-gravity conditions was also conducted using a one-dimensional two-phase flow model. Using slightly modified versions of available correlations for the interfacial friction factor and the turbulent eddy diffusivity, it was found that predictions of this model agreed well with the data obtained over a wide range of conditions. While some useful insight can be gained from experiments of this type, the results of this study indicate that the flow of two liquids of equal density fails to model some important aspects of liquid–vapor two-phase flow at zero gravity. The limitations of this type of experimental simulation are discussed in some detail.

Key Words: two-phase flow, zero gravity, two-phase pressure drop, void fraction, liquid–liquid two-phase flow

1. INTRODUCTION

The power requirements for future spacecraft and satellites are expected to increase as they increase in sophistication and capability. Due to new communications, data processing and surveillance techniques, satellites are planned to operate at power levels of 5–10 kW and future requirements are expected to increase to 100 kW (Mahefkey 1982).

Present thermal control methods are based on the transport of heat by solid conductors and internal radiation, heat pipes and single-phase liquid and gaseous loops. The high operating power levels for future space applications require more efficient thermal transport techniques. Two-phase loops have been suggested and laboratory tested on the earth for possible application in the above areas (Fowle 1981; Ollendorf & Costello 1983). In comparison to a single-phase loop, a two-phase system operates at considerably smaller flow rates and maintains smaller temperature differences with an even higher heat transfer coefficient.

1.1. Background

The design of two-phase heat transport systems for space applications requires a knowledge of the heat and mass transfer processes and fluid mechanics under reduced gravity conditions. Identification of the two-phase flow regimes and determination of the pressure drop, void fraction–quality relation and two-phase heat transfer coefficients are of great importance for the design of two-phase systems.

Current knowledge of two-phase flow and heat transfer is derived primarily from terrestrial experiments. Unlike pool boiling, which has been studied extensively under reduced gravity conditions, little work has been carried out on two-phase flow under reduced gravity conditions due to the difficulty in performing the pertinent tests. Most of the experimental data are from ground-based simulations of very short duration.

1.2. Brief Review of Previous Studies

The subject of two-phase flow and heat transfer has been studied extensively due to its importance in the chemical and nuclear industries (e.g. Hetsroni 1982). Due to the complex nature of two-phase flow, many problems are treated empirically and even fundamental approaches are augmented with empirical factors. The empirical treatment of two-phase flow makes extrapolation to other conditions, e.g. reduced gravity, impractical.

The flow regime transitions of gas–liquid flow systems have been well-studied. Taitel & Dukler (1976) studied the case of horizontal and near-horizontal gas–liquid flow. A study by Charles *et al.* (1961) gave a flow regime map for nearly equal-density oil–water flow. Lovell (1985) investigated the liquid–vapor flow in simulated zero-gravity conditions using two equal-density liquids.

The areas of bubble formation and pool boiling under reduced gravity conditions have been studied extensively. Most of these studies were experimental investigations which were carried out in drop towers (Siegel & Usiskin 1959; Usiskin & Siegel 1961; Siegel & Keshock 1964; Oker & Merte 1973). Some tests have also been performed by simulating reduced gravity conditions, e.g. by compensating for the earth's gravity by using a strong magnetic force (Kirichenko & Charkin 1970; Papell & Faber 1966). The results from pool boiling experiments have shown small changes in the nucleate boiling heat transfer coefficient but a considerable decrease in the critical heat flux with decreasing gravity has been obtained. Bubble formation and departure have been studied by resolution of gravity into components in a tilted (or horizontal) container (Kirichenko & Verkin 1968; Malcotsis 1976).

In contrast to the border effect in the areas of pool boiling, critical heat flux and bubble growth mechanisms, much less work has been done on understanding and modeling two-phase flow at reduced gravities. A review by Siegel (1967) has covered the early reduced gravity studies. Recent reviews of experimental efforts in reduced gravity two-phase flow are given by Anotoniak (1985) and Abdollahian (1988).

Results of experimental studies of pressure and temperature changes in forced convective boiling at zero gravity have been reported by Cochran (1970) and Feldmanis (1966). Low heat flux convective boiling at zero gravity using a drop tower facility was studied by Cochran (1970). This study mainly determined the bubble size and the evaporative layer thickness on the channel walls. The airplane trajectory test results reported by Feldmanis (1966) have shown that the system pressure and temperature increase and boiling oscillations damp out in zero gravity. Studies have reviewed the concept of two-phase flow applications for spacecraft (Fowle 1981; Ollendorf & Costello 1983). These efforts have primarily been qualitative studies of two-phase flow under microgravity conditions.

1.3. Objectives and Scope of Effort

The overall objectives of this study were to generate a data base for the two-phase pressure drop and void fraction–quality under simulated zero-gravity conditions and to develop analytical models to predict their variation under bubbly and annular flow conditions.

A system with two immiscible, nearly equal-density liquids was used to explore the suitability of simulating a gas–liquid system under zero gravity. Water was used as one of the working fluids and simulated the gaseous phase, the second fluid simulated the liquid phase. The ratios of the viscosities and surface tensions of the two liquids were in the range of the two-phase liquid–gas flows. The tests were performed under fully-developed turbulent flow conditions.

The modeling effort is limited to developing relations for the two-phase friction multiplier and void fraction–quality relation under annular flow conditions. The model is based on the triangular approach of Hewitt (1961). The interfacial shear and entrainment relations are empirically determined from the results of the experiments with nearly equal-density liquids.

2. EXPERIMENTAL INVESTIGATION

The experiment was planned to simulate steady-state zero-gravity gas–liquid flow behavior. This was accomplished by using two immiscible liquids of nearly the same density. Proper scaling would

Table 1. Properties at room temperature

Fluids	Viscosity (cSt)	Specific gravity	Surface tension (dyn/cm)	Resistivity (Ω-cm)
Water	0.894	1.0	71.95(water–air)	2×10^4
L-45	10.0	0.938	32.31(water–L-45)	1×10^{14}
DT-LF	4.323	1.038	48.57(water–DT-LF)	6×10^{11}

also require a simulation of the viscosity and interfacial tension ratios. The pressure drop and void fraction at different flow rates were measured in both the annular and bubbly flow regimes. The existence of these two flow regimes was checked by the method of visual verification.

2.1. Selection of Liquids

Due to its abundance, distilled water was chosen to be one of the test fluids. Because of the relatively low viscosity of water compared with other liquids, water simulated the gas in a zero-gravity gas–liquid flow simulation. Since the kinematic viscosity controls the diffusion rate of momentum in the fluid flow, the selection of the simulated liquid phase was based mainly on the ratios of the candidate liquids' kinematic viscosity values to that of the distilled water to be comparable to the same ratio of the water–steam system. The ratio of kinematic viscosity for water to steam at the above-mentioned conditions is about 13. According to the proper kinematic viscosity ratio, equal density and the immiscibility, dimethyl silicone fluid L-45, a product of Union Carbide Corp., and Dowtherm LF heat transfer fluid (DT-LF), Dow Chemical Corp., were chosen to simulate the liquid phase. The properties of the test fluids are listed in table 1. Since the turbulent forces were much greater than the buoyancy forces in these tests, specific gravity values of 0.938 and 1.038 were considered to be sufficiently close to unity for simulating the two-phase flow characteristics under zero-gravity conditions.

2.2. Test Loop and Instrumentation

The experimental apparatus is shown in figure 1. Distilled water and the simulated liquid (L-45 or DT-LF) were pumped from separate storage tanks into a mixing section. Bubbly flow was simulated by introducing distilled water, through 0.4 mm dia holes, in L-45 or DT-LF flow. For annular flow simulation, an annulus with either 1.91 or 0.95 mm clearance was used and water was pumped through the central tube while L-45 or DT-LF flow entered through the annulus. The test

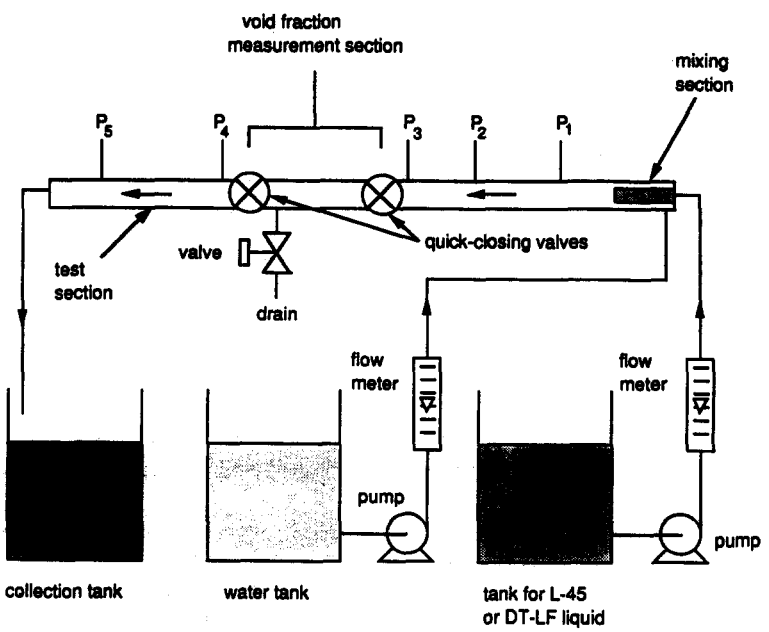

Figure 1. Experimental apparatus schematic. P_1–P_5 are the pressure-sensing points.

Table 2. Test matrix

L-45–water flow				DT-LF–water flow			
Re_t	Min(x)	Max(x)	No. of data points	Re_f	Min(x)	Max(x)	No. of data points
Bubbly Flow Mixing Section				*Bubbly Flow Mixing Section*			
5500	0.13	0.80	13	9000	0.17	0.45	5
7900	0.08	0.68	20	15,900	0.09	0.41	5
8800	0.11	0.51	7	18,000	0.08	0.36	5
10,200	0.07	0.45	5				
11,600	0.11	0.37	5				
Annular Flow Mixing Section (annulus thickness = 0.191 cm)							
6900	0.39	0.84	6				
7900	0.38	0.74	5				
8900	0.40	0.66	5				
(annulus thickness = 0.095 cm)							
5500	0.54	0.79	5				

section was a 3.65 m long, 19.05 mm i.d. round tube which was instrumented to measure the pressure drop and volume ratios of the two-component flow.

The test procedure consisted of running simulated liquid through the whole test section to establish the "liquid-phase" flow condition. Distilled water was then introduced into the simulated liquid flow through the mixing section to produce the desired flow pattern. The proper mass quality was obtained by adjusting the control valves for the two flows. The pressure differences between the first pressure tap and the other four taps were measured. The measurement of the local void (volume) fraction between the third and fourth pressure taps could be carried out in two ways. One was by the impedance probe and the other method was to measure the void fraction of the mixture sample which was obtained directly from the test section during each test run. The data obtained from the impedance probe were compared with that measured directly from the mixture sample to justify the use of the probe.

The system was once-through and the liquids were not circulated in a closed loop. Instead, the mixture was collected in a receiving tank and the liquids were separated under the action of gravity. After the separation had been accomplished, the distilled water was drained and discarded. The simulated liquid was pumped back through a bypass line into its storage tank for future use.

2.3. Test Matrix

The two-phase flow condition in the test was specified in terms of the total Reynolds number (Re_t, based on simulated liquid properties) and the mean phase content or mass quality. The selected Re_t values and mass qualities for L-45–water flow and DT-LF–water flow with the bubbly and annular flow mixing sections are listed in table 2.

2.4. Test Results

2.4.1. Two-phase multiplier

The measured pressure drop was used to calculate the two-phase friction multiplier defined by

$$\phi_L^2 = \frac{\left(\frac{dP}{dz}\right)_F}{\left(\frac{dP}{dz}\right)_L},$$

where $(dP/dz)_F$ is the two-phase frictional pressure gradient and $(dP/dz)_L$ is the frictional pressure gradient for the liquid phase alone.

The calculations were based on the following relation for the single-phase friction factor, obtained from Kays & London (1964):

$$\text{Re} < 2000: \quad f = \frac{16}{\text{Re}}.$$

Define $R = \dfrac{\text{Re}}{1000}$

$$2000 < \text{Re} < 4000: \quad f = 10^{-5}[902 - 304(R-2) + 148(R-2)(R-2.5) - 34.35(R-2)(R-2.5)(R-3)],$$

$$4000 < \text{Re} < 6800: \quad f = 10^{-5}[635 + 90(R-4) - 22.5(R-4)(R-5) + 2.083(R-4)(R-5)(R-6)],$$

$$6800 < \text{Re} < 8000: \quad f = 10^{-5}[782 + 40(R-6.8) - 100(R-6.8)(R-7) + 83.33(R-6.8)(R-7)(R-7.5)]$$

and

$$8000 < \text{Re}: \quad f = 0.05858\,\text{Re}^{-0.2258}$$

where Re is the Reynolds number and f is the friction factor.

The two-phase multipliers vs the inverse Martinelli parameter for different flow conditions are shown in figures 2–6. The Martinelli parameter, X_{tt}, is defined as

$$X_{tt}^2 = \frac{\left(\dfrac{dP}{dz}\right)_L}{\left(\dfrac{dP}{dz}\right)_G} = \frac{\rho_L f_L}{\rho_w f_w}\frac{q_L^2}{q_w^2}, \qquad [1]$$

where $(dP/dz)_G$ is the frictional pressure gradient for the gas phase alone, ρ_L is the density of the liquid, ρ_w is the density of the water (0.997 g/cm^3), f_L is the single-phase friction factor for the simulated liquid, f_w is the single-phase friction factor for the water, q_L is the liquid phase volume flow rate (gpm) and q_w is the simulated gas phase (water) volume flow rate (gpm).

A correlation for the two-phase multiplier as a function of the inverse Martinelli parameter for all the experimental data was obtained as

$$\phi_L = \sqrt{1 + \frac{2.6}{X_{tt}} + \frac{0.1}{X_{tt}^2}}, \qquad [2]$$

and is plotted in figures 2–6. For comparison, Martinelli's correlation for air–water flow (Lockhart & Martinelli 1949),

$$\phi_L = \sqrt{1 + \frac{20}{X_{tt}} + \frac{1}{X_{tt}^2}}, \qquad [3]$$

is also presented in figures 2–6.

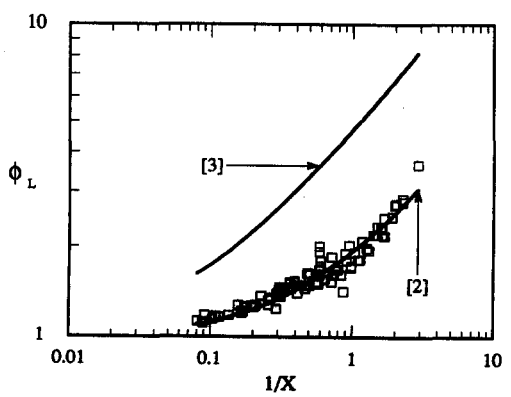

Figure 2. Two-phase friction multiplier vs the inverse Martinelli parameter for all data points.

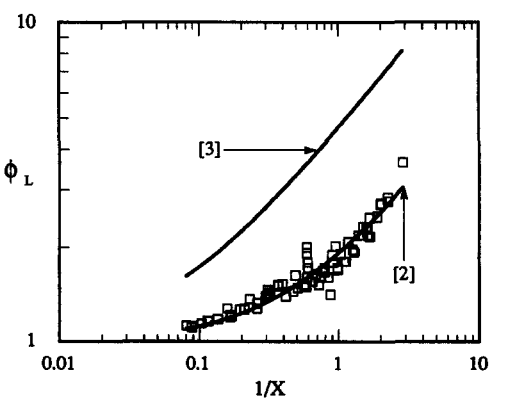

Figure 3. Two-phase friction multiplier vs the inverse Martinelli parameter for L-45–water flow with bubbly and annular flow mixing sections at various Re_t.

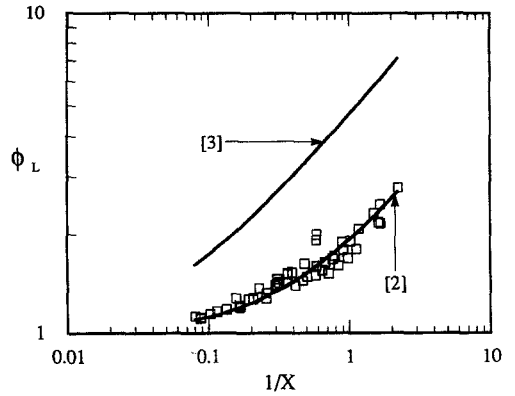

Figure 4. Two-phase friction multiplier vs the inverse Martinelli parameter for L-45–water flow with the bubbly flow mixing section at various Re_l.

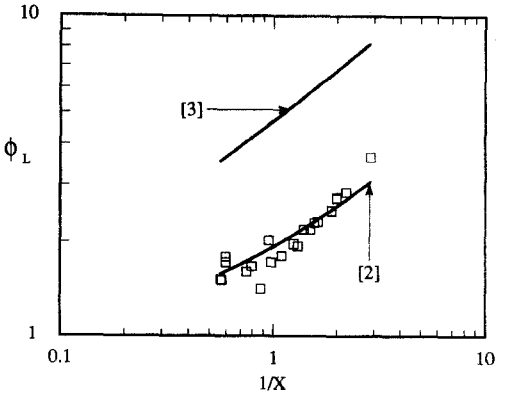

Figure 5. Two-phase friction multiplier vs the inverse Martinelli parameter for L-45–water flow with the annular flow mixing section at various Re_l.

2.4.2. *Void fraction*

The directly measured void fractions are plotted vs the inverse Martinelli parameter for different flow conditions in figures 7–11. The recommended correlation for the void fraction as a function of the inverse Martinelli parameter, based on all the experimental data, is

$$\epsilon = \left[1 + \left(\frac{1}{X_{tt}}\right)^{-1.45}\right]^{-0.8}, \qquad [4]$$

where ϵ is the void fraction, and is plotted in figures 7–11. Martinelli's correlation for the void fraction, based on air–water flow (Lockhart & Martinelli 1949),

$$\epsilon = \left[1 + \left(\frac{1}{X_{tt}}\right)^{-0.8}\right]^{-0.378}, \qquad [5]$$

is also shown in the figures.

2.4.3. *Flow regimes*

Observations of the two-phase mixture sample obtained directly from the test section during each test run before a total separation showed that the fluid sample generally consisted of separated water, L-45 (or DT-LF) and a milky mixture of the above two fluids with foam-like clusters of various grain sizes. The amount of milky mixture decreases with the increase in the directly measured void fraction. When the void fraction was $\leqslant 0.4$, the two-phase sample was mostly a

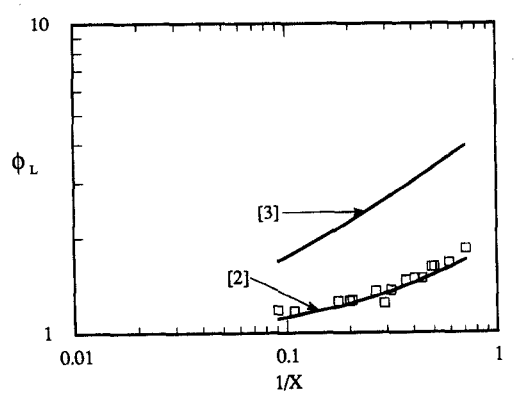

Figure 6. Two-phase friction multiplier vs the inverse Martinelli parameter for DT-LF–water flow with the bubbly flow mixing section at various Re_l.

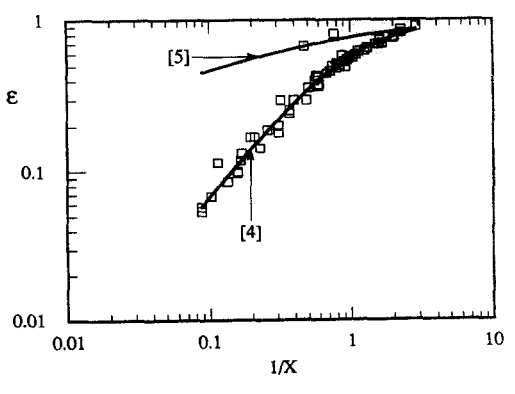

Figure 7. Void fraction vs the inverse Martinelli parameter for L-45–water flow with bubbly and annular flow mixing sections at various Re_l.

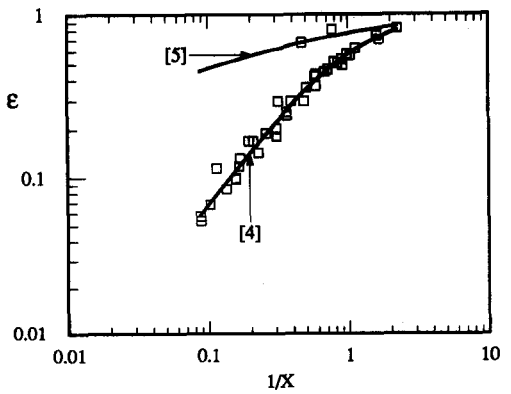

Figure 8. Void fraction vs the inverse Martinelli parameter for L-45–water flow with the bubbly flow mixing section at various Re_t.

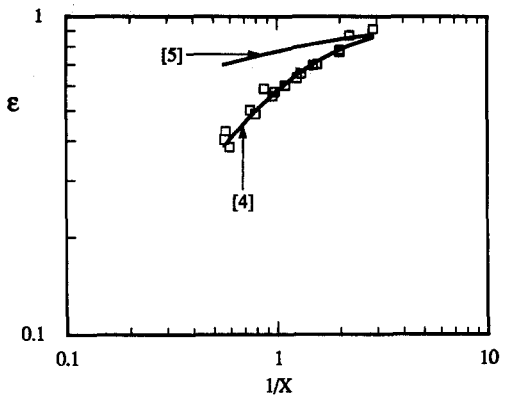

Figure 9. Void fraction vs the Martinelli parameter for L-45–water flow with the annular flow mixing section at various Re_t.

milky mixture with a small amount of L-45 (or DT-LF). When the void fraction was $\geqslant 0.6$, a substantial amount of separated water was observed with some milky mixture and a small quantity of L-45. The foam-like milky mixture formed large grains when the bubbly flow mixing section was used and formed finer grains when the annular flow mixing section was used.

The dominant amount of foam-like milky mixture observed in low void fraction samples suggests a bubbly type of flow [i.e. water drops in L-45 (or DT-LF)]. The appearance of clear separated water in high void fraction samples would appear to imply the existence of an annular type of flow with an L-45 film on the wall and entrainment of small amounts of L-45 in a core flow that is mostly water. The void fraction data taken by the impedance probe agree well with those from the direct measurements in the case of the bubbly flow and deviate significantly from the direct measurement data when the flow apparently becomes annular. This deviation was mainly caused by the poorly conducting (relative to the distilled water) liquid annulus on the inner wall of the test section. Indirectly, this phenonema further suggests our conclusions regarding the existence of the two flow regimes described above.

Our flow regime results do not exactly agree with the flow regime map of Taitel & Dutler (1976), as was also found by Lovell (1985) in his study of a similar equal-density liquids simulation. The results can not be compared with the flow regime map of Charles *et al.* (1961) because it is not clear whether the tendency for droplets to coalesce and the wetting characteristics of their fluids are similar to those of our fluids.

Because our results imply the existence of annular flow for some conditions, an attempt was made to adapt a conventional annular flow model to these circumstances. This aspect of the study is described in the next section.

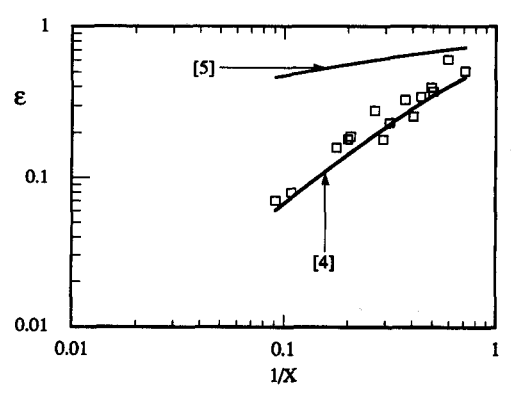

Figure 10. Void fraction vs the inverse Martinelli parameter for DT-LF–water flow with the bubbly flow mixing section at various Re_t.

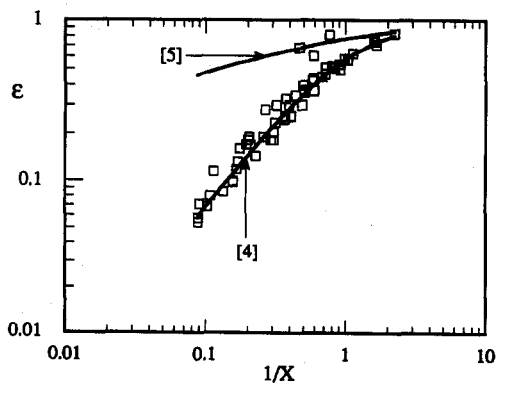

Figure 11. Void fraction vs the inverse Martinelli parameter for all data points with the bubbly flow mixing section.

3. ANALYSIS OF ANNULAR FLOW

It is believed that under annular flow conditions, a significant fraction of liquid may be entrained as droplets in the gas core. There is a continuous interchange of mass and momentum between the liquid film and the gas core. The predictive capability of a phenomenologically based annular flow model rests on the relations used to define the interfacial friction factor and the entrainment fraction.

A one-dimensional steady-state annular flow model is presented. The model uses the triangular relationship proposed by Hewitt (1961) and employs empirical relations for the interfacial friction factors and entrainment fraction. The resulting model provides a method for determining the two-phase friction multiplier and void fraction under annular flow conditions in the absence of buoyancy.

3.1. One-dimensional Steady-state Annular Flow Model

A force balance on the gas core for horizontal steady fully-developed annular flow is given by

$$\tau_i = \tfrac{1}{2} f_i \rho_c u_c^2 = -\frac{r_i}{2}\left\{\frac{\partial P}{\partial z} + \left(\frac{r_o}{r_i}\right)^2 \frac{\partial}{\partial z}\left[G^2\left(\frac{r_o}{r_i}\right)^2 \frac{x^2}{\rho_G}\right]\right\} = -\frac{r_i}{2}\frac{dP}{dz},$$

where τ_i and f_i are the interfacial shear stress and frictional factor, ρ_c and u_c are the mean core density and velocity, r_i and r_o are the radii of the gas core and the tube wall, P is the pressure, z is the axial distance along the flow direction, G is the mass flux, ρ_G is the density of the gas phase and x is the mass quality.

Assuming that the core can be considered as a homogeneous mixture of gas and entrained liquid, ρ_c is given by

$$\rho_c = \frac{\dot{m}_c}{\dot{m}_G}\rho_G = \rho_G\left(1 + \frac{1-x}{x}e\right), \qquad [6]$$

where $\dot{m}_c$ and $\dot{m}_G$ are the mass flow rates of the gas core and the gas phase and e is the equilibrium entrainment fraction. It is also assumed that the ratio of the mass flux in the core to the mass flux within the liquid film is constant, i.e.

$$K = \frac{\dfrac{\rho_G q_G + e\rho_L q_L}{\epsilon_c}}{\dfrac{(1-e)\rho_L q_L}{1-\epsilon_c}}, \qquad [7]$$

where

$$\epsilon_c = \left(1 - 2\frac{\delta}{D}\right)^2$$

is the ratio of the gas core cross-sectional area to the total cross-sectional area of the tube, δ is the film thickness and D is the i.d. of the test section (1.905 cm). Equation [7] can be solved for the entrainment fraction, which results in the following:

$$e = \left[\frac{1-\epsilon_c}{1+(K-1)\epsilon_c}\right]\left(\frac{K\epsilon_c}{1-\epsilon_c} - \frac{\rho_G q_G}{\rho_L q_L}\right). \qquad [8]$$

The mean core velocity is given by

$$u_c = \frac{1}{\rho_c \epsilon_c} G[x + (1-x)e]. \qquad [9]$$

The relation between the void fraction ϵ and ϵ_c can be expressed as

$$\epsilon = \frac{\epsilon_c - e}{1-e}. \qquad [10]$$

Using [6] and [9], the force balance becomes

$$\tau_i^* = \frac{f_i}{2}\frac{x[x+e(1-x)]}{(1-2a)^4}, \qquad [11]$$

where τ_i^* is the nondimensional interfacial shear stress, defined as $\tau/(G^2/P_G)$, and a is the dimensionless film thickness $(=\delta/D)$.

Note that

$$\frac{r_i}{2} = \frac{D-2\delta}{4} = \frac{D}{4}\sqrt{\epsilon_c}$$

and

$$\left(\frac{dP}{dz}\right)^* = -\frac{4}{\sqrt{\epsilon_c}}\tau_i^*, \qquad [12]$$

where $(dP/dz)^*$ is the nondimensional frictional pressure gradient, defined as $(dP/dz)/(G^2/\rho_G D)$.

The relation for the shear stress distribution in the liquid film given by Hewitt (1961) is

$$\tau(r) = \tau_i\left(\frac{r_i}{r}\right) + \frac{1}{2}\frac{dP}{dz}\left(\frac{r_i^2 - r^2}{r}\right),$$

where r is the radial distance measured from the centerline of the test section and $\tau(r)$ is the shear stress at r, which can be expressed as

$$\tau^* = \tau_i^*\left(\frac{1-2a}{1-2a\eta}\right) + \frac{1}{4}\left(\frac{dP}{dz}\right)^*(1-2a\eta)\left[\left(\frac{1-2a}{1-2a\eta}\right)^2 - 1\right], \qquad [13]$$

where τ^* is the nondimensional shear stress, defined as $\tau/(G^2/\rho_G)$, η is the dimensional distance $(=y/D)$ and y is the radial distance measured from the tube wall into the flow.

From the shear stress expression in the liquid film we obtain

$$\frac{du}{dy} = \frac{\tau}{\mu_L + \alpha_t \rho_L}, \qquad [14]$$

where u is the mean velocity, α_t is the dimensionless turbulent eddy diffusivity and μ_L is the viscosity of the liquid phase, and

$$\frac{du^*}{d\eta} = \mathrm{Re}_L\, a\frac{\tau^*}{1+\dfrac{\alpha_t}{\nu_L}}, \qquad [15]$$

where u^* is the nondimensional mean velocity, defined as $u/(G/\rho_w)$, and ν_L is the kinematic viscosity of the liquid phase.

The nondimensional total liquid film mass flow rate $\dot{M}$ is defined as

$$\dot{M} = \frac{4\dot{m}_L}{\pi D^2 G} = 4a\int_0^1 (1-2a\eta)\gamma u^*\, d\eta, \qquad [16]$$

where $\dot{m}_L$ is the mass flow rate of the liquid phase and γ is the ratio of the liquid density to the simulated gas (water) density. For each guessed value of δ (or equally, a) the calculated $\dot{M}$ can be compared with the given nondimensional liquid film mass flow rate:

$$\dot{M} = (1-x)(1-e). \qquad [17]$$

When the two values for $\dot{M}$ are equal, the film thickness is obtained.

The two-phase multiplier in section 2.4.1. can be related to the nondimensional quantities as follows:

$$\phi_L^2 = -\frac{\gamma\left(\frac{dP}{dz}\right)^*}{2f_L(1-x)^2}. \qquad [18]$$

3.2. Procedure for Calculating the Film Thickness, Two-phase Multiplier and Void Fraction

The film thickness can be obtained by iteration as follows:

(1) Given flow conditions G, x and fluid properties, a value for the dimensionless liquid film thickness, a is assumed.
(2) Using the correlation for the interfacial friction factor, f_i and [11], τ_i^* is evaluated.
(3) Equations [11] and [12] are used to calculate $(dP/dz)^*$.
(4) The relation for eddy diffusivity along with [13] are used to integrate [15] from $\eta = 0$ to $\eta = 1$ to obtain u^* for different η values.
(5) Equation [16] is used to calculate the liquid film mass flow rate, $\dot{M}$.
(6) The values of $\dot{M}$ calculated from [16] and [17] are compared and the above steps are repeated to satisfy both equations.
(7) With a correct value of a, the Martinelli parameter, X_{tt}, void fraction, ϵ, and the two-phase multiplier, ϕ_L^2, can be obtained from [11], [12] and [18].

3.3. Interfacial Friction, Entrainment Rate and Eddy Diffusivity Correlations

As mentioned earlier, the accuracy of the physically based annular flow models rests on the correlations used for the interfacial friction and entrainment rate. Wallis (1970) suggests the following relation for the interfacial friction factor:

$$f_i = f_s\left(1 + 300\frac{\delta}{D}\right),$$

with a value of 0.005 for f_s. Whalley & Hewitt (1978) use

$$f_i = f_s\left[1 + 24\left(\frac{\rho_L}{\rho_G}\right)^{1/3}\frac{\delta}{D}\right]. \qquad [19]$$

Different models for the entrainment rate have been proposed but no satisfactory correlation is presently available.

For calculating the velocity profile in the liquid film, Hewitt (1961) used Deissler's relation, while Levy & Healzer (1980) used the mixing length approach. The model described in section 3.1. was used to predict the two-phase friction multiplier and cross-sectional average void fraction for the conditions tested with L-45–water. Different relations for the interfacial friction, entrainment fraction and eddy diffusivity were tested and the following relations gave the best agreement.

3.3.1. Interfacial friction factor

An exponential variation with the film thickness was found to yield better agreement than the generally used linear relation

$$f_i = 0.005\exp\left(\frac{\delta}{D}\right).$$

3.3.2. Entrainment fraction

Although a constant ratio of mass flux between the core and liquid film is not physically correct, it was found that the constant K in [7] is a weak function of the film thickness and flow rates. A value of K = 0.95 was used in [8] to obtain the entrainment fraction.

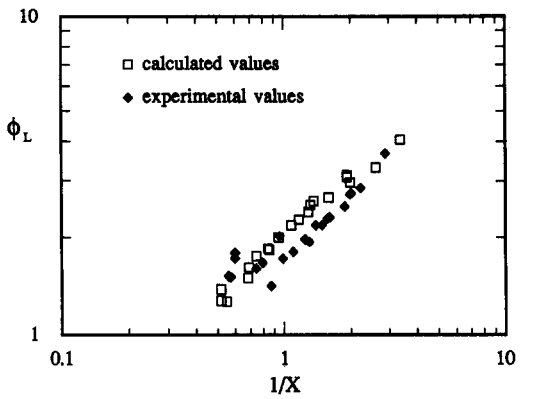

Figure 12. Comparison of the calculated values for the two-phase friction multiplier with the experimental values.

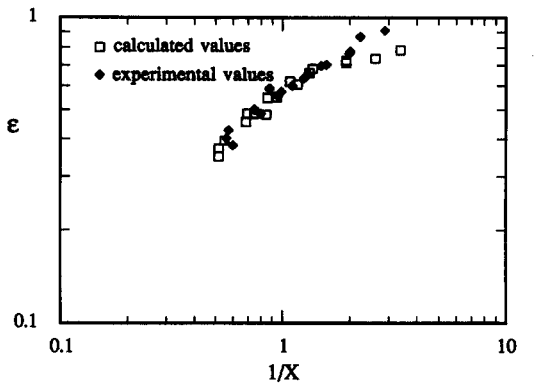

Figure 13. Comparison of the calculated values for the void fraction with the experimental values.

3.3.3. *Eddy diffusivity*

The following nondimensional turbulent eddy diffusivity was used in the present model:

$$\frac{\alpha_t}{\nu_L} = 0.16\left[y^+\left(1-\frac{y^+}{y_0^+}\right)\right]^2\left[1-\exp\left\{-\left[\frac{0.16y^+\left(1-\frac{y^+}{y_0^+}\right)}{20}\right]\right\}\right],$$

where

$$y^+ = \left(\frac{y}{D}\right)\left(\frac{GD}{\mu_L}\right)\left(\frac{f_L}{2}\right)^{1/2} \quad \text{and} \quad y_0^+ = \frac{\delta G}{\mu_L}\left(\frac{f_L}{2}\right)^{1/2}.$$

3.4. *Comparison with the Experimental Data*

The calculated two-phase multipliers and the experimental data for L-45–water flow with the annular flow mixing section are shown in figure 12. The calculated void fractions and the experimental data for the same flow conditions are shown in figure 13. As expected, the predictions compare well with the experimental data since the empirical relations were developed from the same data base. It is noted, however, that the model does not result in good agreement with pressure drop data for the nitrogen/water tests by Cuta (1987). The interfacial friction and entrainment rates are empirically developed from the experiments with two equal-density liquids. As will be discussed in section 4, the method of simulating reduced gravities with two liquids for annular flow conditions is questionable. Although the model provides a general approach for predicting annular flow pressure drop and void fraction under reduced gravities the empirical relations should be modified for use with gas–liquid flow in the absence of gravity.

An attempt was made to modify the empirical relations. A density ratio was introduced in the interfacial friction relation to make it applicable to different fluid combinations. The same density ratio was used by Whalley & Hewitt (1978). This modification made the predictions more reasonable, but the entrainment rates were considerably higher than expected and the resulting two-phase multipliers were higher than the measured values by a factor of 2. This result could have been expected, since the correlation for the entrainment rate is based on the data for two liquids which have a smaller interfacial tension than gas–liquid flows. Previous studies have shown that the entrainment rate increases with decreasing surface tension. In addition, visual observations during the experiment showed considerably higher entrainment than expected with gas–liquid systems. One could reduce the entrainment rate by the ratio of interfacial tensions or vary the constant K in [8] to improve the agreement with the reduced gravity data. However, the limited amount of data do not justify such a modification at the present time. The above approach with the density correction introduced in the interfacial friction relation shows promising trends but more reduced gravity gas–liquid data are needed to develop a correlation for entrainment.

4. CONCLUSIONS

(1) In order to develop a better understanding of two-phase flow behavior under reduced gravity conditions and generate a data base for the two-phase pressure drop and void–quality relation, an experimental program was developed to simulate these conditions. These tests provide data for long duration steady-state fully-developed two-phase flow conditions.

(2) The simulation of zero gravity by using two nearly equal-density liquids also depends on other properties of the gas–liquid system; the wetting capability of the liquids as well as the relative viscosities and surface tensions are particularly important. However, as will be discussed in points (3) and (4) below, the fact that the density difference between the gas and liquid is small makes it difficult to quantitively simulate the annular flow case.

(3) The test matrix was selected to result in turbulent flow conditions. The simulation of zero-gravity two-phase flow under turbulent conditions is more appropriate for bubbly flow. This is due to the fact that in a two-liquid annular flow condition, the liquid which represents the gas phase travels at a velocity which is not greatly different from the average velocity of the other phase. However, in a gas–liquid annular flow, the phases travel at considerably different velocities due to the density difference. As a result, the two-liquid annular flow simulation can only provide a qualitative representation of the actual conditions by eliminating the buoyancy effects.

(4) The annular flow model was based on a phenomenological approach and resulted in good agreement with the data. However, since the empirical relations used for the interfacial friction and the entrainment rate are based on the data from the equal density liquids, they may not be directly applicable to a gas–liquid flow in zero gravity. The model does, however, provide a general approach for predicting annular flow pressure drop and void fraction. Attempts to generalize the empirical relations for gas–liquid flow at reduced gravities showed promising trends but more tests are needed to develop relations for the interfacial friction and entrainment rates.

(5) It was observed that in the liquid flows studied here, small, foam-like bubble clusters are more likely to form rather than large, discrete bubbles. This suggests that bubbles tend to be more thoroughly dispersed in the zero-gravity condition, which is consistent with the observations of Karri *et al.* (1988).

Acknowledgements—This research was sponsored by the Flight Dynamics Lab., Air Force Wright Aeronautical Labs., U.S. Air Force. The authors gratefully acknowledge the support and appreciate the detailed review of the technical manager, Mr. William Haskin.

REFERENCES

ABDOLLAHIAN, D. 1988 Study of two-phase flow and heat transfer in microgravity. Final Phase I Report SLI-8802.

ANOTONIAK, Z. I. 1985 Two-phase alkali–metal experiments in reduced gravity. Report PNL-5906.

CHARLES, M. E., GOVIER, G. W. & HODGSON, G. W. 1961 The horizontal pipeline flow of equal density oil–water mixtures. *Can. J. chem. Engng* **39**, 27–36.

COCHRAN, T. H. 1970 Forced convection boiling near inception in zero gravity. NASA TN D-5612.

CUTA, J. 1987 Personal communication with D. Abdollahian. Pacific Northwest Lab.

FELDMANIS, J. C. 1966 Pressure and temperature changes in closed loop forced convection boiling and condensing processes under zero gravity conditions. *Proc. Inst. envir. Sci.* **8**, 455–461.

FOWLE, A. A. 1981 A pumped, two-phase flow heat transport system for orbiting instrument payload. In *Proc. AIAA 16th Thermophysics Conf.*, Paper 81-1075.

HETSRONI, G. 1982 *Handbook of Multiphase Systems*. Hemisphere, Washington, D.C.

HEWITT, G. F. 1961 Analysis of annular two phase flow: application of the Dukler analysis to vertical upward flow in a tube. Report AERE-R3680.

KARRI, S. B., REDDY & MATHUR, V. K. 1988 Two-phase flow regime map predictions under microgravity. *AIChE Jl* **34**, 137–139.

KAYS, W. M. & LONDON, A. L. 1964 *Compact Heat Exchangers*, 2nd edn. McGraw–Hill, New York.

KIRICHENKO, Y. A. & CHARKIN, A. I. 1970 Studies of liquid boiling in imitated reduced gravity fields. In *Proc. 4th Int. Heat Transfer Conf.*, Vol. 6, p. B8.9.

KIRICHENKO, Y. A. & VERKIN, B. I. 1968 Simulation of zero and reduced gravity fields for heat transfer investigations under boiling. *Dopov. Akad. Nauk ukr. RSR Ser. A* 7.

LEVY, S. & HEALZER, J. M. 1980 Prediction of annular liquid–gas flow with entrainment—cocurrent vertical pipe flow with no gravity. EPRI Report NP-1409.

LOCKHART, R. C. & MARTINELLI, R. C. 1949 Proposed correlation of data for isothermal two-phase two-component flow in pipes. *Chem. Engng Prog.* **45**, 39–48.

LOVELL, T. K. 1985 Liquid–vapor flow regime transition for use in the design of heat transfer loops in spacecraft: an investigation of two phase flow in zero gravity conditions. AFWAL Report TR-85-3021.

MAHEFKEY, T. 1982 Military spacecraft thermal management: the evolving requirements and challenges. AIAA Paper 82-0827.

MALCOTSIS, G. 1976 The mechanism of bubble detachment from a wall at zero and negative gravity. *J. Fluid Mech.* **77**, 313–320.

OKER, E. & MERTE, H. 1973 Transient boiling heat transfer in saturated liquid nitrogen and F-113 at Stanford and zero gravity. Final Report NASA-20228.

OLLENDORF, S. & COSTELLO, F. A. 1983 A pumped two-phase system for spacecraft. Presented at the *13th Intersociety Conf. on Environmental Systems*, Paper SAE 831099.

PAPELL, S. S. & FABER, O. C. 1966 Zero and reduced gravity simulation on a magnetic–colloid pool-boiling system. Report NASA TND-3288.

SIEGEL, R. 1967 *Effects of Reduced Gravity on Heat Transient. Advances in Heat Transfer*, Vol. 4. Academic Press, New York.

SIEGEL, R. & KESHOCK, E. G. 1964 Effects of reduced gravity on nucleate boiling bubble dynamics in saturated water. *AIChE Jl* **10**, 509–523.

SIEGEL, R. & USISKIN, C. M. 1959 A photographic study of boiling in the absence of gravity. *Trans. ASME Jl Heat Transfer* **81**, 230–236.

TAITEL, Y. & DUKLER, A. E. 1976 A model for predicting flow regime transitions in horizontal and near horizontal gas–liquid flow. *AIChE Jl* **22**, 47–54.

USISKIN, C. M. & SIEGEL, R. 1961 An experimental study of boiling in reduced and zero gravity fields. *ASME Jl Heat Transfer* **83**, 243–253.

WALLIS, G. B. 1970 Annular two-phase flow, part 2—additional effects. *J. basic Engng* **92**, 73–82.

WHALLEY, P. B. & HEWITT, G. F. 1978 The correlation of liquid entrainment fraction and entrainment rate in annular two-phase flow. Report AERE-R9187.